Research Article

A Vascular-Network-Based Nonuniform Hierarchical Fault-Tolerant Routing Algorithm for Wireless Sensor Networks

Hongbing Li,[1,2] Peng Gao,[1] Qingyu Xiong,[3] Weiren Shi,[1] and Qiang Chen[2]

[1] *School of Automation, Chongqing University, Chongqing 400030, China*
[2] *School of Computer Science and Engineering, Chongqing Three Gorges University, Chongqing 404100, China*
[3] *School of Software Engineering, Chongqing University, Chongqing 400030, China*

Correspondence should be addressed to Hongbing Li, sxxylhb@163.com

Fault tolerance is the key technology in wireless sensor networks which attracts many research interests. Aiming at the issue that the nodes' failures affect the network's stability and service quality, a vascular-network-based fault-tolerant routing algorithm is presented by nonuniform hierarchical clustering. According to the distribution characteristics of the vascular network and inspirations to the fault tolerance for wireless sensor networks, a mathematical model and network topology are, respectively, established. It applies the improved particle swarm optimization (IPSO) to the nonuniform hierarchical clustering, and multipaths are established between the neighbor hierarchical nodes based on the best-worst ant system (BWAS). It introduces the normalized values of the pheromone generated by the ants as the selection probabilities of transmitting paths to establish the hierarchical routing. Theoretical analysis and simulations show that the algorithm has higher packet receiving rates, lower average transmission delay, and balanced energy consumption. It has the good performance in fault tolerance and stability of data transmitting, and it avoids the hot issue in energy consumption and achieves the network load balance.

1. Introduction

Due to the characteristics of dynamic variation of the topology, no center ad hoc network and the constraints of the resources in wireless sensor networks (WSNs), as well as the unpredictability of the working scenario, such as the vibration and electromagnetic interference, it is prone to unbalance of energy consumption, poor quality of data transmission, and routing instability [1, 2]. So they have great influence on the key technologies, including average transmission delay, packet receiving rate, and average energy consumption, which closely correlate with the network's stability, accuracy, and reliability. They also weaken the reserved function and bring greater challenges to the existing network technologies, especially for the application in the complex scenario and necessity for strict performance, just like condition monitoring for key facilities and poisonous gas, emergency, and disaster releasing.

The network with good performance should have the integrity of the fault features, the accuracy of fault diagnosis, and fault recovery efficiency. It can perform well in the robustness of nodes' interconnection, accuracy of data transmission, and against the fast energy consumption as well as the malicious invasion. It also can make a timely diagnosis, find a reasonable control decision, and continue to provide high-credibility computational services by adaptively handling the anomalies of the network. Fault tolerance is the key technology in wireless sensor networks which has attracted great attention and becomes a hot issue that needs further study [3].

Fault tolerance in wireless sensor networks is a complex system problem which includes fault prevention, detection, isolation, diagnosis, and recovery [3]. It mainly includes the optimization of each layer's protocols or algorithms and joints optimal control among multilayer and hardware fault tolerance [4–6]. Fault tolerance in the network layer [7] and

collaborative optimization among the layers are to be the important direction. Fault tolerance in the network layer is to explore the mechanism of multirouting data transmission [7], network coding [8], and so on. The mechanism of multirouting data transmission is to reestablish a path or select one from the multirouting table established in advance to realize the fault tolerance when the source node confirms that the fault exists in the transmitting routing, namely, the redundancy routing fault tolerance [9–11]. Network coding is to transmit the encoded data along multipaths and realize the fault tolerance by decoding and reconstructing the data at sink node, that is, the redundant data fault tolerance [12–14]. The combination of a variety of fault-tolerant methods or collaborative optimization with other layers will achieve the good result [7, 15]. The mechanism of multipath data transmission and network coding improves the stability of data transmission and network load balance. However, it increases the computational complexity, transmission delay, and energy consumption.

Fault tolerance based on the principle of bionics and modern intelligent bionic algorithms has recently been attracting growing research interests in the study of wireless sensor networks. They include biological immune system mechanism, the fuzzy diagnosis, the expert system, the artificial neural network, the particle swarm optimization, ant colony algorithm, and genetic immune algorithm. They provide good ideas and methods to the fault-tolerance and show better fault tolerant effect in wireless sensor networks. For example, the ant colony algorithm with the advantage of swarm intelligence is introduced into the routing establishment in the network layer; the particle swarm algorithm is introduced into the topology establishment with its characteristics of fast clustering convergence to improve the efficiency of clustering; artificial neural network or its combination with the fuzzy algorithm is applied to forecast the perception data to realize fault tolerance in the application layer; genetic algorithm can be applied to the data unit coding to improve fault tolerance of the data transmission in the link layer or network layer.

It has already shown the good performance and advantages when introducing the mechanism of biological immune system into the fault tolerance in wireless sensor networks [16–23]. Some basic research works have been done in this aspect. Bokareva et al. have presented a fault-tolerant architecture SASHA based on the biological immune system, in which the lymph mechanism is used to produce the detector for fault detection, and the thymus mechanism is used to complete the fault diagnosis. This structure cannot only identify the known fault model, but also provide a good adaptive ability of learning and evolving to the unknown fault model [16]. Jabbari and Lang apply the mechanisms of biological immune system to the security detection and fault tolerance by simulating the mechanisms of self-learning, self-organization, and memory and information processing in the biological immune system or the nerve immune system [17]. Atakan and Akan propose the new distributed node and rate selection method (DNRS), which is based on the principles of natural immune system to select the minimum number of sensor nodes based on the B-cell stimulation in immune system to transmit the data to the sink and select the appropriate reporting frequency of sensor nodes to achieve the minimum energy consumption [18]. Rui et al. propose an immune system inspired approach to locally discover and recover from losses of query messages at sensor nodes, similar to antibodies in an immune system [19]. Chen et al. propose a neighborhood node selection algorithm to decide if a sensor node is activated or not according to the B-cell and T-cell models of immune systems by comparing the similarity between artificial immune system and wireless sensor networks [20]. Hu et al. present a hybrid routing scheme and an immune cooperative PSO algorithm for fault-tolerant routing problem [21]. In [22], uniform immunization and temporary immunization are conducted on small worlds of tree-based wireless sensor networks to combat the sensor viruses. Salmon et al. propose an intrusion detection system (IDS) framework inspired by the human immune system to monitor their neighborhood and to identify an intruder [23]. Mechanism of biological immune system or immune algorithms can also be applied in routing optimization, intrusion detection, nodes' deployment, target coverage, and performance optimization.

This paper will explore establishing the nonuniform hierarchical clustering based fault-tolerant routing algorithm by the bionic intelligent algorithms according to the characteristics of vascular network and inspiration to fault tolerance based on the preliminary studies. It will carry out the fault tolerance studies by combining the routing establishment with the topology design to improve the network's performance of stability and reliability. The main work and contribution of this paper is: (1) to study the structure and characteristics of the vascular network and the inspirations to the fault tolerance and to establish the mathematical model and network topology; (2) to study the IPSO and BWAS, making these intelligent algorithms more optimal and more suitable for resource-restrained network; (3) to study the nonuniform hierarchical static clustering by applying the IPSO; (4) to study the routing establishment by applying the BWAS.

It innovatively establishes the hierarchical fault-tolerant topology based on the vascular network and uses the normalized values of the ants' pheromone as the selection probability of the transmission paths to establish the fault-tolerant routing by improved intelligent algorithms. Deference with previous studies in the methods of fault tolerance in the network layer is not to simultaneously establish multipaths or backup paths for each relay node, but to temporarily select the path with maximum normalized values of the pheromone between the two neighbor hierarchical nodes to establish the optimal transmission route. If this node fails, then it selects the other node as the substitute, in which the path is with the second maximum normalized values of the pheromone as the backup transmission path to realize the fault tolerance. The new reestablished transmission path is not from the source node to sink node but from the node ahead of the fault node to the sink node by the selection probability. Furthermore, the intelligent algorithms are improved to fit for the source-restrained network.

The rest of this paper is organized as follows. Section 2 studies the mathematical model of the vascular network and topology. Section 3 presents the nonuniform hierarchical clustering algorithm based on the improved particle swarm optimization (IPSO) and the fault-tolerant routing algorithm by the best-worst ant system (BWAS). Section 4 carries out the simulations and analysis to evaluate the performance. Finally, Section 5 concludes the paper and discusses the future work.

2. Mathematical Model and Network Topology

2.1. Mathematical Model. The vascular network is the fractal tree-like branching network. It has the complex structure with the characteristics of the fractal [24]. Great differences exist among the different sections of the vascular in the structures, physical characteristics, and functions. Different sections have different blood flowing rate. It has the properties of stability, flexibility, connectivity, and multiconnectivity. Blood flows in the directed way according to the pressure difference that exists between any two points. Blood flow has quantitative relationship with current velocity, cross-section, and the pressure.

The characteristics of the vascular network give an important inspiration to the establishment of fault-tolerant routing in WSN. The nodes are hierarchically marked to have the hierarchy differences according to distance to sink node to ensure the directed data transmission. Different clustering probabilities are adopted in different hierarchical areas. Finally, it forms the distribution with different density and scale of the clusters in different hierarchical areas, which has a similar topology with the vascular network model. The vascular-network-based topology has multipaths connectivity and uses the pheromone normalized values generated by ants in ant colony algorithm as the path selection probability to establish the optimal transmission routing to realize the fault tolerance.

The vascular-network-based mathematical model has the following characteristics. (1) Pressure differential network. Each node in WSN has the differential pressure value P', which reflects the distance to center node of the network. The ones closer to the center node have higher pressure values. So the pressure difference $\Delta P'$ exists between any two nodes, which reflects the directed data flow. (2) Connectivity of the weighted graph; it is the directed weighted graph and each side is assigned with the different weights $w(e)$. Any two points in the network are connected. (3) Clustering density. Different quantity and density of the clusters are presented in different hierarchies. Larger quantities and higher distribution density of the clusters are presented in the areas with smaller hierarchy values. The mathematical formulations are as follows:

$$P'_i > P'_j, \quad \text{if } dist(i, s') < dist(j, s'), \ i, j \in (1, 2, \ldots, n),$$

$$\Delta P'_{i,j} = p'_i - p'_j, \qquad \vec{p'_i} = \sum \vec{p'_i},$$

l is the neighbor node of i,

$$p'_i = \frac{r}{dist(i, s')},$$

$$a_{ij} = \begin{cases} w_{ij}, & (v_i, v_j) \in E, \\ 0, & i = j, \\ \infty, & (v_i, v_j) \notin E, \end{cases}$$

$$(1)$$

where P'_i is the pressure of node i, $\Delta P'_{i,j}$ is the pressure difference between the nodes i and j, $dist(i, s')$ represents the Euclidean distance from the node i to center node s', n is the quantity of the clustering nodes of network, r is a parameter value, $\vec{p'_i}$ represents the directed pressure, a_{ij} is the adjacent matrix element of directed weighted graph, and E is the set of side (i, j).

2.2. Network Topology

Definition 1. Hierarchy: nodes in WSN are marked with different hierarchies according to the distance from the average node to sink node. The nodes belonging to the same hierarchical area are marked with the equal hierarchy value, that is,

$$G_i = m \quad \text{if } dist(s, i) \in ((m - 1)r, mr), \tag{2}$$

where G_i represents the hierarchy value of the node i, $dist(s, i)$ represents the Euclidean distance from the node i to sink node s, and r is the initial distance value.

2.2.1. Nonuniform Hierarchical Clustering Topology. The topology is established based on the theory and characteristics of vascular network. (1) The nodes in the network are divided into two categories: the average nodes and clustering nodes. Average nodes are responsible for data collection and transmission. Besides this, clustering nodes have the functions of data receiving, forwarding, and routing addressing. The network routing is established among the clustering nodes. (2) The network is divided into different hierarchies by the distance to the sink node. The nodes in the same hierarchical area have the same hierarchy value, and the routing is established among the clustering nodes with different hierarchies. (3) It is the directed weighted graph with connectivity between any two nodes in the network. Each link has different weight; the data propagation and message broadcasting have directions according to the nodes' pressure gradient. (4) Different quantity and scale of the clusters are presented in different hierarchical areas. Larger quantity and smaller scale of the clusters are presented in the areas with smaller hierarchy values and so does the opposition in the areas with higher hierarchy values. (5) Multipaths will be established between the nodes that are the neighbor hierarchical within their transmission power coverage. The normalized values of the pheromone are used as the probabilities to select the transmitting path. The link with maximum probability is to be selected as the transmitting path. The established physical topology of network is shown in Figure 1.
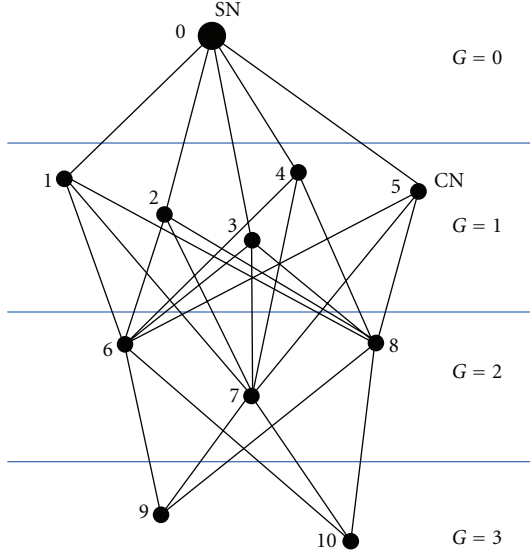
FIGURE 1: Physical topology of the network.

Figure 1 shows the network's topology based on the vascular network. It is divided into 3 hierarchies. Node 0 is the sink node, and nodes 1–10 are the clustering nodes. The nodes 1–5 in hierarchy 1 are responsible for the data fusion, receiving the data from the nodes in hierarchy 2 and retransmitting the data to the sink node. Nodes 6–8 in hierarchy 2 are responsible for data fusion in their respective clusters and retransmitting the data from nodes in hierarchy 3 to nodes in hierarchy 1. Nodes 9 and 10 in hierarchy 3 are only responsible for the data fusion and transmitting the data to the nodes in hierarchy 2. For example, node 7 in hierarchy 2 will establish the transmission path with nodes 1–5 in hierarchy 1 and nodes 9-10 in hierarchy 3 within its transmission power coverage excluding the nodes 6 and 8 which belong to the same hierarchy. And the value w_{ij} of each side is not equal.

The fault tolerance of the topology is owing to the normalized value of the ants' pheromone used as the selection probability of the transmission path, and it selects the path with the maximum probability as the transmission path. For example, the pheromone on the links connecting the node 7 in hierarchy 2 with the nodes 1–5 in hierarchy 1 is different, that is, $\tau_{7,3} \geq \tau_{7,2} \geq \tau_{7,4} \geq \tau_{7,1} \geq \tau_{7,5}$, where τ represents the normalized pheromone value. Therefore, the real transmitting path is Path$_{7,3}$. When this path fails, it will select the path with the second maximum probability as a substitute. If Path$_{7,3}$ fails, Path$_{7,2}$ is to be selected.

2.2.2. Establishing Rules. The topology will be established based on clustering model. The nodes are functionally divided into average nodes (ANs) and clustering nodes (CNs). The routing is established among the hierarchical clustering nodes. The clustering node is to establish the transmission paths only with neighbor hierarchical nodes, not the same hierarchical ones. It establishes the transmission path with all the neighbor hierarchical nodes within

the transmitting power coverage. Only one path is to be selected as the actual transmission one, and the rest are the backup transmission paths. The establishing rule is shown in Algorithm 1.

2.2.3. To Determine the Clustering Probability. Different clustering probabilities are adopted in different hierarchical areas to form the different scale and quantity of the clusters, which means nonuniform clustering. Clustering node is dynamically selected according to the residual energy to balance the energy consumption in one cluster [25, 26].

The network is separated into different annular sections with the sink node as the center and $n \cdot R$ ($n \in 1, 2, \ldots$) as the radius. The nodes in the same annular section have the same hierarchy value. It applies the larger clustering probability in hierarchy 1 where it is close to the sink node and smaller clustering probabilities in the hierarchical areas that are far from it. It eventually forms the distribution with large quantity and smaller scale of the clusters that are closer to the sink node, as shown in Figure 2.

This topology based on the vascular network model can balance the energy consumption and avoid the hot issue. However, how to determine the clustering probability in each hierarchical area becomes the key issue. The energy consumption model refers to [27], the radius of each area is $n \cdot R$, and the total number of the nodes is $N_{n \cdot R}$ that the network is divided into n areas. The clustering probability is p_n ($n \in 1, 2, \ldots$) for the area where the radius is R. The number of the clusters is $N_{n \cdot R} \cdot p_n$ in each area. The number of the nodes in one cluster is $1/p_n - 1$ excluding the clustering node. Suppose each node only sends data k bit, so the energy consumption of the clustering node is as follows:

$$
\begin{aligned}
E_{R \cdot \text{clu}} &= E_{\text{fuse}}\left(\frac{1}{p_1} - 1\right)k + E_{\text{elec}}(n-1)k \\
&\quad + E_{\text{elec}}(k + (n-1)k) \\
&\quad + \varepsilon_{\text{amp}}(k + (n-1)k)d^2, \\
&\qquad\qquad i \in \left(1 \cdots (N_{n \cdot R} p_i)\right) \\
&= E_{\text{fuse}}\left(\frac{1}{p_1} - 1\right)k + E_{\text{elec}}(2n-1)k \\
&\quad + \varepsilon_{\text{amp}} n k d^2.
\end{aligned}
\tag{3}
$$

The energy consumption of the nodes excluding the clustering nodes is as follows:

$$
E_{R \cdot \text{ave}} = E_{\text{elec}}\left(\frac{1}{p_1} - 1\right)k.
\tag{4}
$$

The whole energy consumption in one cluster is as follows:

$$
E_{R \cdot \text{total}} = \sum_{1}^{N_R p_1} (E_{R \cdot \text{clu}} + E_{R \cdot \text{ave}}).
\tag{5}
$$

In order to minimize the energy consumption, from $\partial E_{R \cdot \text{total}}/\partial p_1 = 0$, we can get p_1. According to $E_{R \cdot \text{total}} = E_{2R \cdot \text{total}}$ for the balance of energy consumption, we can get p_2, and so on.

Suppose $G_k = G_{k+1} = \cdots = G_{k+l} = m,\ i \neq i',\ i, i' \in (k, k+1, \ldots k+l)$;
$G_i = G_{i'} = m,\ i \neq i'$;
If $G_j = \{m-1, m+1\},\ j \in (k', k'+1, \ldots k'+l')$;
   If $\text{Dist}(i, j) > \text{Dist}RF$;
      $i \not\rightleftharpoons j$;
   else
         $i \rightleftharpoons j$;
      end
end

Where $\text{Dist}(i, j)$ represents the Euclidean distance of node i and j, $DistRF$ represents the nodes' RF distance. G_k represents the hierarchy of node k. $\not\rightleftharpoons$ shows that it cannot establish the transmission path.

ALGORITHM 1: Establishing rules of non-uniform hierarchical topology.
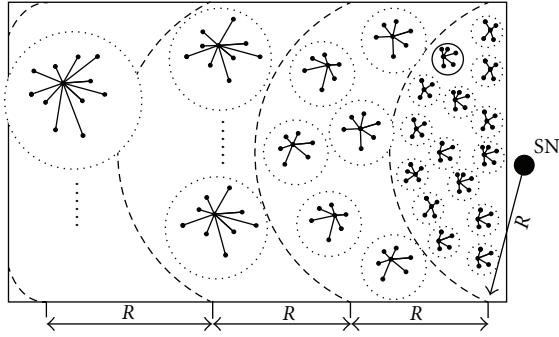

FIGURE 2: Nonuniform hierarchical static clustering.

3. Nonuniform Hierarchical Clustering Routing

3.1. Nonuniform Hierarchical Clustering Strategy. Particles, with equal quantity of the nodes, are randomly deployed in the active hierarchical area. It does the initial $N_{n \cdot R} \cdot p_n$ clustering by clustering probability and then introduces the IPSO to intelligent clustering. It modifies the particles' flying rules when the particles move to the location coinciding with the sensor nodes, the location of the particle becomes fixed and the velocity turns to zero. The particles no longer follow the rule that the particles' velocities and locations are updated by their own and swarms' optimum. The rest particles continue to fly by established rules until the whole particles' locations coinciding with sensor nodes. It forms the optimal clustering distribution and then turns to the next hierarchical area.

3.1.1. PSO Prototype. PSO is an optimization algorithm based on swarm intelligence which imitates birds' behavior. Swarm intelligent optimization searching is carried out by the cooperation and competition of the particles. Each solution of the generation has the characteristics of learning the optimum of itself and the group. Each particle is determined by its position and velocity vector. Each particle confirms them by the established direction as well as experiences from

the optimal direction of itself and the swarm's. The velocity and location is updated by the following formulae:

$$v_i^{t+1} = w v_i^t + c_1 r_1 \left(p\text{best}_i^t - x_i^t \right) + c_2 r_2 \left(g\text{best}_j^t - x_i^t \right), \quad (6)$$

$$x_i^{t+1} = x_i^t + v_i^{t+1}, \quad (7)$$

where the inertia weight coefficient $w = w_{\max} - (w_{\max} - w_{\min}) \cdot k/m$ is the linear descending function by time. It can make PSO explore the larger area at the beginning and roughly locate the position faster. With w descending gradually, the particles' speed gets slower and begins to locally search subtly. $w_{\max}$, $w_{\min}$ are, respectively, the initial and eventual weight, m is the maximum iterations, k is the current iterations, v_i^t is the particle's velocity vectors, and x_i^t is the particle's current position, r_1, r_2 are random numbers between 0 and 1 to keep the diversity of the group, c_1, c_2 are the learning factors which make it keep the ability of self-summary and learning from the optimal particles, and $p\text{best}_i^t$ and $g\text{best}_j^t$ are, respectively, the best positions of the particle itself and the swarm.

3.1.2. IPSO

(a) Modify the PSO formula with inertia weight. The particles $G = \{x_1, x_2, \ldots, x_m\}$ are divided into k clusters of particle swarms C_i $(i = 1, 2 \ldots, k)$. Modify the formula (6) into

$$V_i^{t+1} = w V_i^t + c_0 r_0 \left(p\text{best}_i^t - X_i^t \right)$$
$$+ \sum_{j=1}^{k} c_j r_j \left(g\text{best}_j^t - X_i^t \right). \quad (8)$$

It updates the particles' position and velocity by the formulae (7) and (8) in each iteration.

(b) Modify particles' flying rules. The particles no longer follow the rule that the particles' velocities and locations are updated by their own and swarms' optimum. In the improved way, when the particle moves

to the location coinciding with the sensor nodes, the particle's location becomes fixed and the velocity turns to zero. The rest particles continue to fly by established rules until the whole particles' locations coincide with sensor nodes. It forms the optimal clustering distribution, and then the clustering is to be carried out in the next hierarchical area.

3.1.3. Steps of the Algorithm

Step 1. Divide the network into different hierarchies by the distance from the nodes to sink node. It uses different clustering probabilities for different hierarchical areas. It selects the nodes in hierarchy 1 as the active nodes and makes others as dormant ones in order to avoid the particles flying into other hierarchical areas.

Step 2. Randomly generate the number of the particles $M = N_{n \cdot R}$ as same as nodes and do the initialization. Define the initial position x_i and flying velocity v_i of each particle, the learning factor c_0, c_j $(j = 1, 2, \ldots, k)$, the inertia weight $w_{\max}$, $w_{\min}$, the maximum speed $v_{\max}$, the maximum position $x_{\max}$, and the maximum m.

Step 3. Determine the number of the clusters $k = N_{n \cdot R} \cdot p_n$ and cluster center c_i in C_i. Each particle swarm has $D = M/k$ dimensions, and different individual particles have different positions.

Step 4. Set the target function to evaluate the fitness of the particles and the clustering quality by Euclidean distance:

$$S = \frac{1}{\sum_{i=1}^{K} \sum_{x \in C_j} dist(c_i, x)^2}, \qquad (9)$$

where the *dist* is the normative Euclidean distance between two objects, K is the number of the clusters, x is the particle, and c_i is the center of cluster C_i.

Step 5. Calculate the particle's self-optimal position $p\text{best}_i^t$ in C_i and the optimal position $g\text{best}_j^t$ of C_i.

Step 6. Judge the particles' positions. When the particle moves to the sensor nodes' position, set $v_i = 0$, $x_i = x_{\text{sensor}}$, where x_{sensor} represents the sensor node's position.

Step 7. Update the rest particles' positions and velocities by formulae (7) and (8).

Step 8. Repeat Steps 3 to 7 until the last particle coincides with the last sensor node. The clustering is over in this hierarchy, and the nodes turn to the dormant state.

Step 9. Wake up the nodes in the hierarchical area $(n - 1)R < \text{dist}(x_{\text{senor}}, x_{\sin k}) < nR$, $n \in (2, 3, \ldots, n)$ and do the clustering by Steps 2 to 8.

3.2. Routing Establishment Based on BWAS.

BWAS is the improvement of the ant colony algorithm. It introduces the rewards-punishment mechanism to magnify the pheromone between the best and worst ants. It improves the ability of the optimal path searching and the convergence rate. And pheromone generated by ants is an important parameter reflecting the path's optimization. It considers the nodes' energy, inspiration of the nodes' distance, and the advantages of swarm intelligence.

Now suppose some artificial ants are set at each clustering node and they will die when finishing searching the paths from the clustering nodes to the sink node. The ants have the memory of the pheromone on the paths passed by.

Step 1. Initialize the parameters; to determine the clustering nodes, set ants' quantity at each clustering node and define their property.

Step 2. Select the path for each ant by formulae (10) and (11):

$$p_{ij}^k(t) = \begin{cases} \dfrac{\tau_{ij}^{\alpha}(t)\eta_{ij}^{\beta}(t)}{\sum_{s \in \text{allowed}_k} \tau_k^{\alpha}(t)\eta_{is}^{\beta}(t)}, & j \in \text{allowed}_k \\ 0, & \text{otherwise}, \end{cases} \qquad (10)$$

$$\tau_{ij}(t + n) = \rho_1 \tau_{ij}(t) + \Delta\tau_{ij}(t, t + n), \qquad (11)$$

$$\Delta\tau_{ij}(t, t + n) = \sum_{k=1}^{m} \Delta\tau_{ij}^k(t, t + n), \qquad (12)$$

$$\Delta\tau_{ij}^k(t, t + n) = \begin{cases} \dfrac{Q}{L_k}, & \text{if ant } k \text{ passes } (i, j) \text{ in this ciculate}, \\ 0, & \text{otherwise}, \end{cases} \qquad (13)$$

where p_{ij}^k is the transition probability of ant k, j is the unvisited node, τ_{ij} is the pheromone intension on side (i, j), η_{ij} is the visibility of the side (i, j) which reflects the inspiration transferring from node i to j, and allowed_k is the node set that the ant is allowed to visit. Formula (11) is to update the pheromone when the ant has finished establishing the whole path, and Q is a parameter.

Step 3. Update the pheromone on the generated paths by formula (14) after each ant finishes the task:

$$\tau_{rs} \longleftarrow (1 - \rho)\tau_{rs} + \rho\Delta\tau_{rs}, \qquad (14)$$

$$\Delta\tau_{rs} = (nL_{nn})^{-1}, \qquad (15)$$

where τ_{rs} represents the pheromone value on the side (r, s), ρ is a parameter, $0 < \rho < 1$, n is the quantity of the nodes, and L_{nn} is the length of the path.

Step 4. Execute Step 2 and Step 3 until each ant generates a path and evaluate the best and worst ants according to the length of the paths passed by.

Step 5. Globally update the pheromone on the paths passed by the best ants by formula (16):

$$\tau_{rs} \longleftarrow (1 - \alpha)\tau_{rs} + \alpha\Delta\tau_{rs}, \tag{16}$$

$$\Delta\tau_{rs} = \begin{cases} \left(L_{gb}\right)^{-1}, & \text{if } (r,s) \in \text{global best}, \\ 0, & \text{otherwise}. \end{cases} \tag{17}$$

Step 6. Globally update the pheromone on the paths passed by the worst ants by the following formula:

$$\tau(r,s) = (1 - \rho)\tau(r,s) - \varepsilon\frac{L_{\text{worst}}}{L_{\text{best}}}, \tag{18}$$

where ε is a parameter, L_{best} and L_{worst} are the lengths of the paths, respectively, passed by the best and worst ant, L_{gb} is the length of global optimal path, and α is the volatilizing parameter of the pheromone, where $0 < \alpha < 1$.

Step 7. Execute Steps 2 to 7 for ants in the rest clustering nodes until all the ants finishes task and record the pheromone values on the paths.

After the hierarchical dividing and static clustering, it uses the normalized pheromone as the selection probability to establish the fault-tolerant routing. When the energy consumption of the clustering nodes reaches the threshold value, they report the information along the established route in order to reduce the energy consumption. When the transmission cycle is over, it selects the nodes with higher energy as the clustering nodes in the clusters. Then, the whole network calculates the new pheromone values of the paths based on BWAS to establish a new routing.

4. Simulation and Analysis

4.1. Simulation on Nonuniform Hierarchical Clustering

4.1.1. The Distribution of Hierarchical Nodes. Assumptions: (1) the nodes in the network are stationary. (2) The locations of the nodes are known. (3) All nodes have the same status and parameters. (4) Each node works at full-duplex operation mode. (5) The nodes distribute uniformly in the rectangular areas, and the sink node is outside.

The simulation is based on PC with processor i3-2100, RAM with 4 G. 150 nodes are deployed in the area [100, 100], the number of hierarchies is $n = 3$, and the initial coordinate of sink node is (120, 50). The radius $R = 40$. The inertia weight coefficient w in IPSO is linearly down from 0.9 to 0.4. The learning factors $c_0 = 1.5$, $c_j = 2$; the quantity and scale of the particle swarm are determined by the clustering probability. The maximum iteration m is set by the experiments to ensure that the last particle's location coincides with the sensor node. r_0, r_j are the random values in [0, 1], and $K = N_{n \cdot R} \cdot p_n$.

Figure 3 shows that 150 sensor nodes are deployed randomly in [100, 100], which are labeled with blue color. These nodes are not hierarchically divided, and all have the equal hierarchical property. The sink node is deployed at (120, 50) and is labeled with red color. The nodes in Figure 4
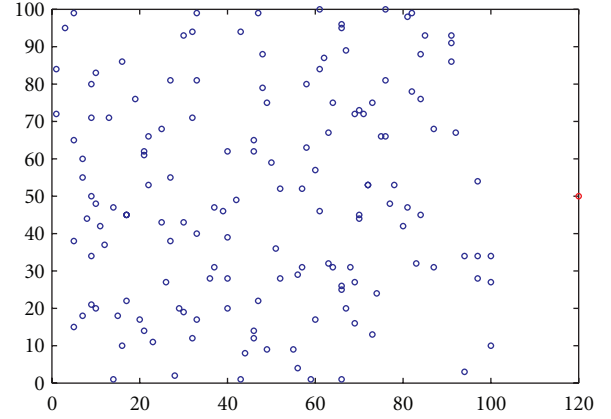

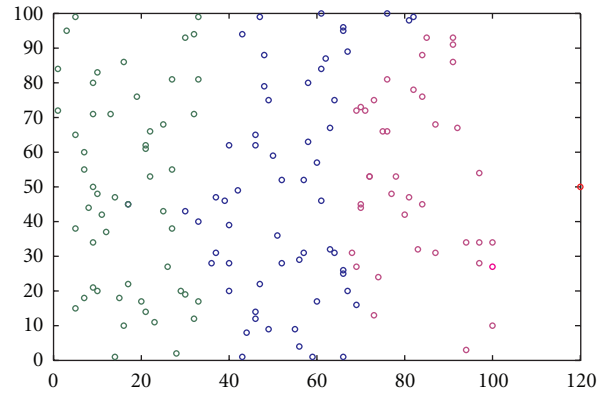FIGURE 3: Nonhierarchical nodes in WSN.

FIGURE 4: Hierarchical nodes in WSN.

are hierarchically divided based on Figure 3. With the sink node as the center of the circle and the distance to sink node as the radius, 3 hierarchical areas are divided, respectively, marked by the colors red, blue, and green. The red nodes belong to hierarchy 1; the blue and green nodes, respectively, belong to hierarchies 2 and 3.

4.1.2. Nonuniform Hierarchical Clustering. The nodes are hierarchically clustered by the IPSO; different clustering probabilities are adopted in different hierarchical areas. Finally, it forms the cluster distribution with different scales and quantities, as shown in Figures 5 and 6.

Figure 5 shows the equal probability hierarchical clustering by IPSO with 3 hierarchies. 150 nodes are clustered by the same probability. The scales of clusters are the same, and there are about 2–4 nodes in each cluster. Figure 6 shows the nonequal probability hierarchical clustering by IPSO with 3 hierarchies. So it forms the distribution that different scales and quantity of clusters are in different hierarchical areas. It, at last, forms the distribution with smaller scales and larger amount of the clusters in the lower hierarchical level where it is near to sink node. And so does the opposition in hierarchy 3 where it has the larger scales of clusters and fewer nodes in each one. It reaches the expected clustering structure.
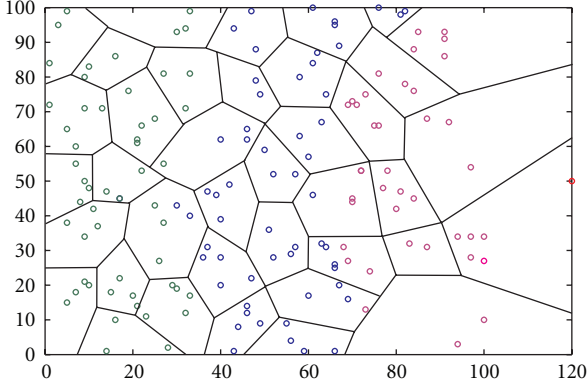
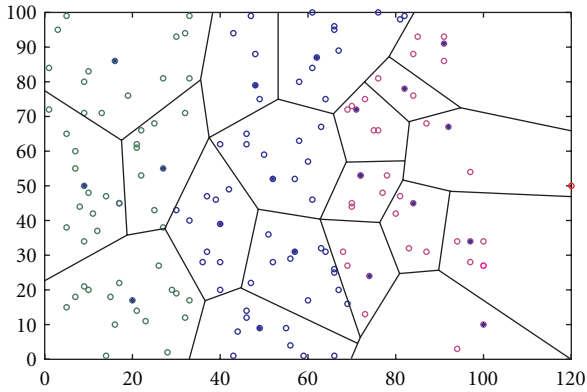FIGURE 5: Equal-probability hierarchical clustering.

FIGURE 6: Nonequal-probability hierarchical clustering.

Table 1 shows the statistics of the nonuniform hierarchical clustering by IPSO. From it, the number of the nodes in hierarchy 1 is 38, the clustering probability is 0.237, and the number of the clustering is 9. According to the energy balance method presented above, we can calculate the probabilities of the second and third hierarchies; they are, respectively, 0.100 and 0.070. The simulation results show the corresponding values are 0.103 and 0.074. From the clustering probabilities, the number of the clusters, and member nodes, we can get the conclusion that the distribution of the clusters is the same with the topology previously supposed.

4.2. Simulation on Nonuniform Hierarchical Clustering Routing

4.2.1. Parameters Setting. After the hierarchical division and nonequal probability static clustering, to place the ants at each clustering node with the number $k = 30$, the initial pheromone value $\tau = 100$. Pheromone inspiration factor $\alpha = 1$; it indicates the relative importance of the pheromone when the ants select the forward way. Expect heuristic factor $\beta = 5$, indicating the relative importance of visibility and affecting the algorithm's convergence rate. The greater the value is, the closer it is to be greedy algorithm according to the state transition probability. Set the pheromone

TABLE 1: Statistics of the nonuniform hierarchical clustering.

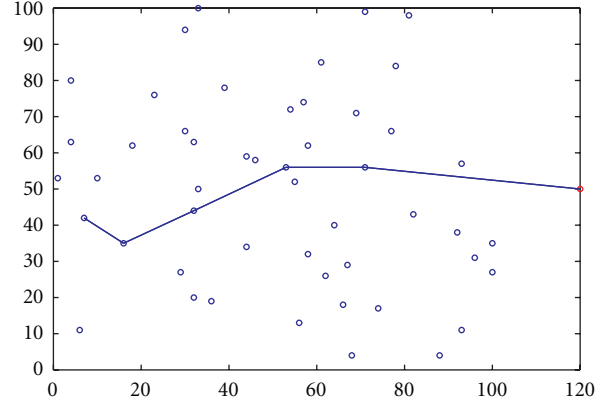| Hierarchy	Hierarchy 1	Hierarchy 2	Hierarchy 3
Number of nodes	38	58	54
Number of clusters	9	6	4
Number of members	29	52	50
Probability of clustering	0.237	0.103	0.074

FIGURE 7: Transmission route from node $(7, 42)$ to sink node.

evaporation coefficient $\rho = 0.1$, pheromone residual factor $1 - \rho$, and the maximum iterations $NC\_\max = 200$.

4.2.2. Process of Routing Establishment. Now we use A to E to identify hierarchies 1 to 5. (x_I, y_I) represents the coordinate of the nodes in hierarchy I, ρ' represents ant's pheromone normalized value. Table 2 shows the normalized values of the ants' pheromone by BWAS on the paths from the node $(7, 42)$ in E to sink node. The node $(7, 42)$ is randomly selected to establish a transmission path from it to sink node. $\rho'_{E \to D}$ represents the normalized values on the paths from the node $(7, 42)$ in E to nodes in D. Table 3 shows the nodes' coordinates corresponding with the normalized values in Table 2. $\rho' = 0.3034$ represents the normalized values of the pheromone on the path from the node $(7, 42)$ to $(x_D, y_D) = (16, 35)$.

From all the normalized values of the ants' pheromone on the paths from the node $(7, 42)$ in E to the nodes in D, $\max \rho' = 0.3034$. So the node $(x_D, y_D) = (16, 35)$ is to be selected as the next hop to establish the transmission route. If the node $(16, 35)$ fails, it will select the path with $\rho' = 0.1515$; therefore, $(x_D, y_D) = (18, 62)$ is to be selected as the next hop. So a routing for data transmission has been set up from node $(7, 42)$ in E to sink node. The hierarchy order of the established path is $E \to D \to C \to B \to A \to$ sink node, and the corresponding order of nodes' coordinates is $(7, 42) \to (16, 35) \to (32, 44) \to (53, 56) \to (71, 56) \to$ sink node, as shown in Table 3. Figure 7 shows that the actual transmission route is established among 50 clustering nodes based on Table 2.

4.2.3. Simulation on the Routing Establishment. Simulation is completed when all the ants reach the sink node by

TABLE 2: Normalized values of the ants' pheromone.

$\rho'_{E \to D}$	$\rho'_{D \to C}$	$\rho'_{C \to B}$	$\rho'_{B \to A}$
0.3034	0.1814	0.1285	0.1162
0.1515	0.1033	0.0873	0.0742
0.0920	0.1469	0.1277	0.1029
0.1299	0.1300	0.0796	0.1254
0.1041	0.0683	0.1086	0.0510
0.0608	0.1188	0.0983	0.0868
0.1039	0.1039	0.0619	0.0601
0.0544	0.0881	0.0889	0.0710
—	0.0729	0.0726	0.0360
—	—	0.0578	0.0525
—	—	0.0461	0.0375
—	—	0.0426	0.0564
—	—	—	0.0454
—	—	—	0.0409
—	—	—	0.0438

TABLE 3: Node's coordinates on the paths.

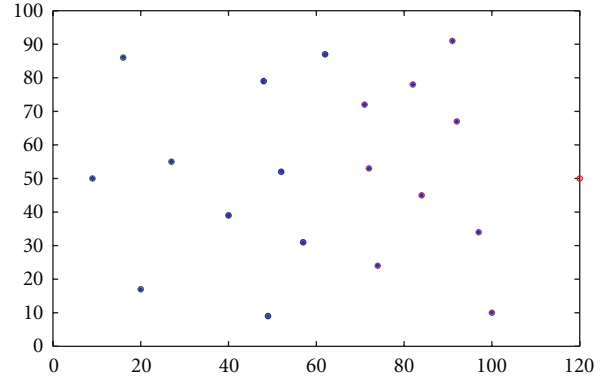| (x_E, y_E)	(x_D, y_D)	(x_C, y_C)	(x_B, y_B)	(x_A, y_A)
(1, 53)	**(16, 35)**	(32, 63)	**(53, 56)**	(64, 40)
(4, 63)	(18, 62)	**(32, 44)**	(54, 72)	(67, 29)
(4, 80)	(23, 76)	(33, 50)	(55, 52)	(69, 71)
(6, 11)	(29, 27)	(36, 19)	(57, 74)	**(71, 56)**
(7, 42)	(30, 66)	(39, 78)	(58, 32)	(74, 17)
(10, 53)	(30, 94)	(44, 34)	(58, 62)	(77, 66)
—	(32, 20)	(44, 59)	(61, 85)	(78, 84)
—	(33, 100)	(46, 58)	(62, 26)	(82, 43)
—	—	(56, 13)	(66, 18)	(88, 4)
—	—	—	(68, 4)	(92, 38)
—	—	—	(71, 99)	(93, 11)
—	—	—	(81, 98)	(93, 57)
—	—	—	—	(96, 31)
—	—	—	—	(100, 27)
—	—	—	—	(100, 35)

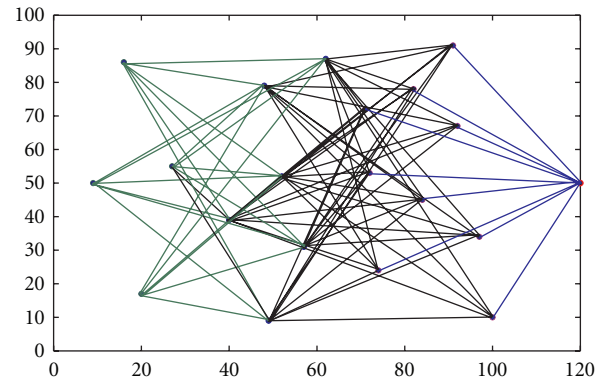FIGURE 8: Clustering nodes in three hierarchies.

FIGURE 9: Paths among the clustering nodes in three hierarchies.

Figure 10 shows the distribution of 50 clustering nodes in five hierarchies. Figure 11 shows all the possible transmission paths among the clustering nodes. We also mark the hierarchical transmission paths with five different colors for distinction. There are five hierarchies for the established paths; the node only establishes the links to the nodes in the neighbor hierarchies. It has an important significance to the quick establishment and optimization of the transmission routing for large-scale network.

4.3. Performance and Complexity Analysis of the Fault Tolerance

4.3.1. Performance Analysis of the Fault Tolerance. (1) Pheromone, generated by ants during the process of searching the optimal path, is an important parameter reflecting the path's quality. The higher τ is, the greater probability the path is selected as transmitting path. (2) It uses the normalized pheromone values as the selectionprobabilities of the paths and selects one with maximum probability as the actual data transmitting path. Any clustering node will establish the possible paths to the nodes in neighbor hierarchies within its transmission power coverage. But only the path with maximum probability is to be selected as actual data transmitting path. If it fails, the path with second maximum probability is to be selected to realize the fault tolerance.

BWAS. The pheromone on each path stops evaporating and is recorded. Node visited by ants is not hierarchical, only by this can pheromone reflect the links' quality.

Figure 8 shows the distribution of the clustering nodes in three hierarchies. According to the nonequal probability clustering method, 19 clustering nodes are elected from total 150 nodes and marked with three different colors as for three hierarchies. Simulations in Figure 9 illustrate that all the possible transmission paths are established among the clustering nodes. Paths in different hierarchy are marked with different colors for distinction. The paths established in Figure 9 show the hierarchical characteristic clearly.

For fewer clustering nodes in WSN, we can more clearly understand the establishment of the transmission paths. However, better performance can be reflected for the large-scale network, as shown in Figures 10 and 11.
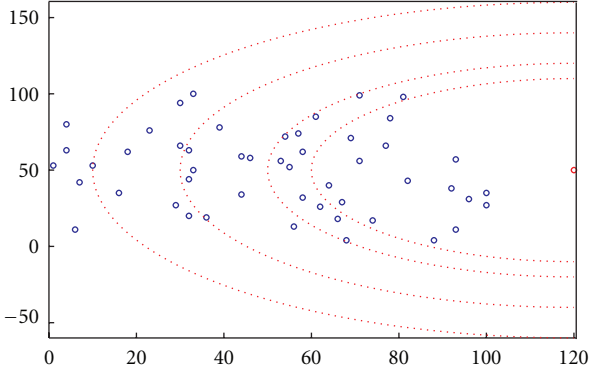
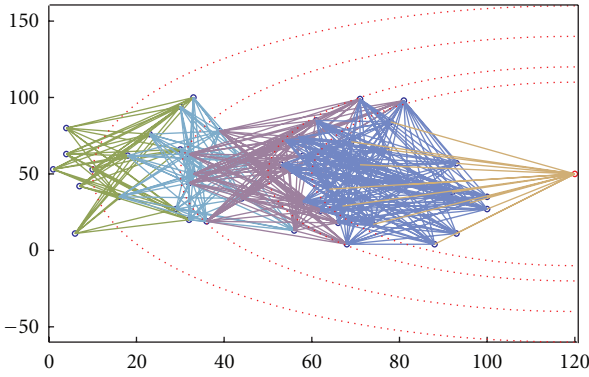FIGURE 10: Clustering nodes in five hierarchies.

FIGURE 11: Paths among the clustering nodes in five hierarchies.

Node 7 in Figure 1, for example, has established the paths path_{7i} ($i = 1, 2, \ldots, 5$) with the nodes 1–5 in the neighbor hierarchy. The normalized values of pheromone are not equal, like $\tau_{7i} \neq \tau_{7j}$ ($i \neq j$, $ij = 1, 2, \ldots, 5$). And the respective selection probabilities are not equal, like $p_{7i} \neq p_{7j}$. So the actual transmission path is $\text{Path}_{7i} \rightarrow \max(p_{7i})$, $i = 1, 2, \ldots,$ 5. If this path fails, it will select $\text{Path}_{7j} \rightarrow \max(p_{7j}, j \neq i,$ $i, j = 1, 2, \ldots, 5)$ as the actual transmission path and so on. The direction of the gathered data transmitting to sink node is $G_3 \rightarrow G_2 \rightarrow G_1$ and opposite direction for the message broadcasting. (3) The method of multipaths establishment is different from others. When the fault occurs, the newly established transmission route reestablishes the route not from the source node to sink node but from the node ahead of fault node to the sink node by the selection probability. It saves the computational complexity and overhead. (4) The fault tolerance of the network is greatly related with the transmission range of the nodes. The larger the transmission range is, the better is the performance of the network; however, the more the energy consumption. The node's transmission range based on the nonuniform hierarchical clustering routing should be set in $[R, 2R]$, where R is the radius of the ring in Section 2.2.3. The node with transmission range in $[R, 2R]$ can cover some nodes in the neighbor hierarchical area and select the best node in the transmission rang coverage to establish the links. It considers the fault tolerance of the network as well as the energy consumption by reasonable transmission range.
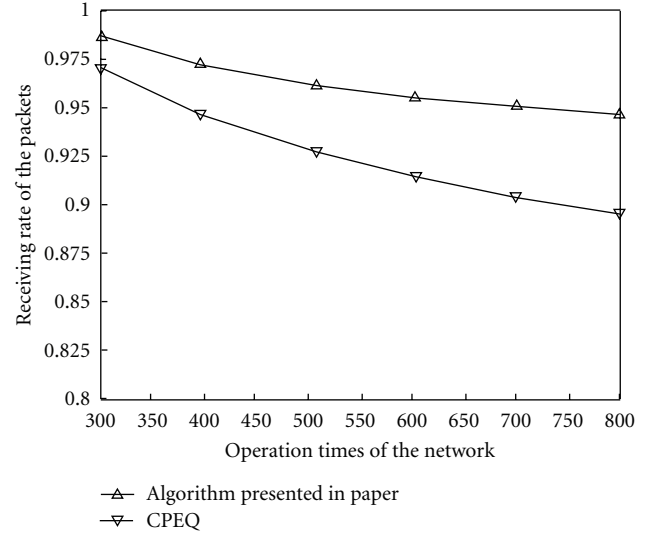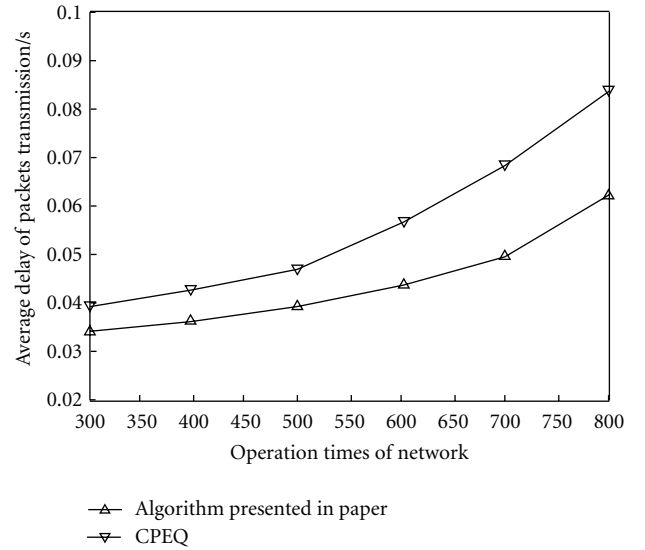

FIGURE 12: Comparison of packet receiving rate.

FIGURE 13: Comparison of average packet transmission delay.

4.3.2. Complexity Analysis of the Algorithm. The computational overhead of the nonuniform hierarchical clustering based fault tolerant routing algorithms is in terms of nonuniform hierarchical clustering by IPSO and computing the pheromone of each path by BWAS. k particle swarms are generated in the process of nonuniform hierarchical clustering by IPSO, and each particle swarm contains $D = M/K$ individual particles; so the computing complexity of the IPSO is $o((M/k)(M/k)d^2d^2k + d^2(M/k)k + k^2d^2) = o((M^2/k)d^4 + k^2d^2)$. When the positions of the particles are gradually becoming consistent with the sensors', the number of active particles becomes less during the process of the clustering. Its computational complexity presents exponential decreasing with the reduction of the number of individual particles, not keeping the same computational complexity from the beginning to the end of the clustering
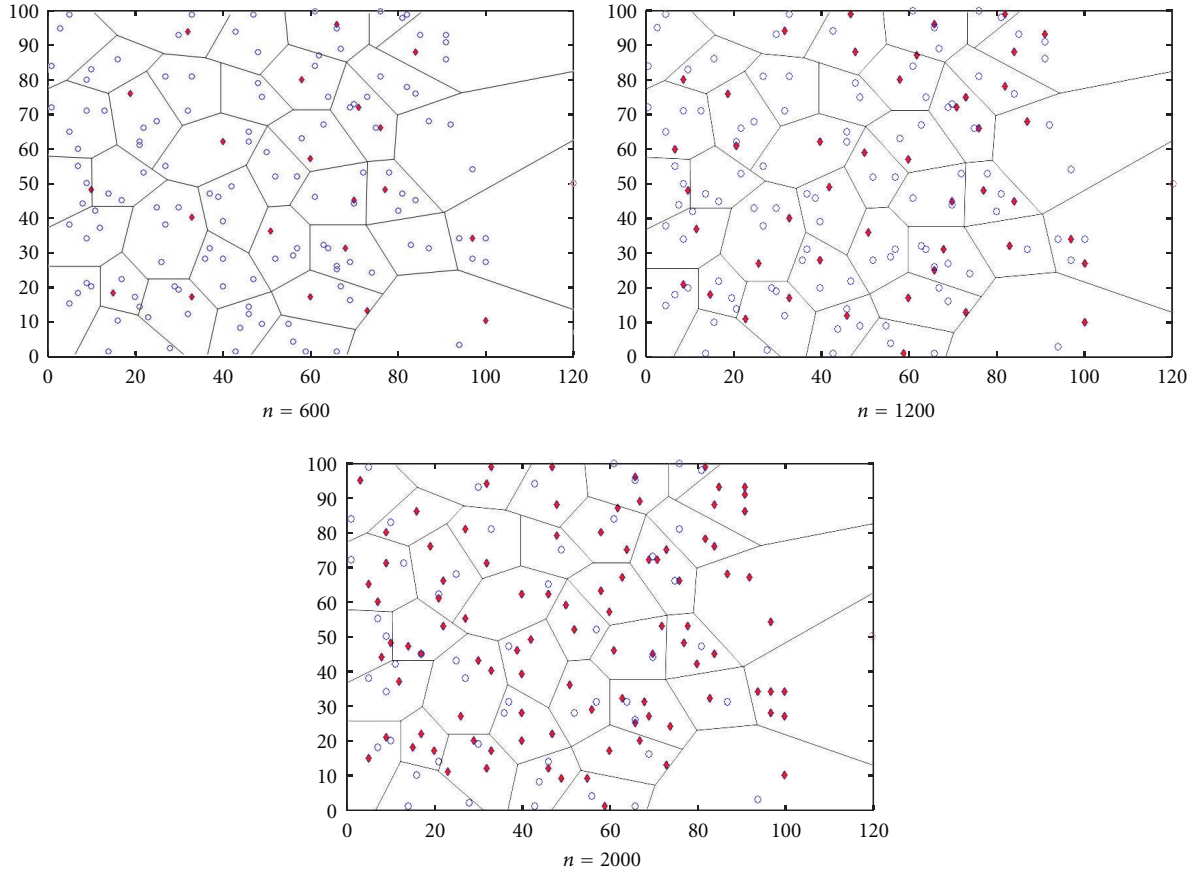
FIGURE 14: Energy consumption by equal probability and nonhierarchical clustering.

by the IPSO algorithm. This is much important to the resource-restricted wireless sensor networks and presents the advantages of the IPSO when using it to cluster in wireless sensor networks.

It has $\sum_{n=1}^{N} N_{nR}$ average nodes and $\sum_{n=1}^{N} N_{nR}p_n$ clustering nodes in wireless sensor networks; so the time complexity of establishing the routing and computing the pheromone of each path is $o(N(\sum_{n=1}^{N} N_{nR}p_n)^3)$ by the improved ant colony algorithm BWAS, where N is the number of iterations, and n is the number of the clustering nodes in each hierarchies. The computing and time complexities are determined by the scale of the network and the selection probability of cluster head nodes as well as the number of iterations.

4.4. Analysis of Receiving Rate and Average Packet Delay. It is important to select the high-quality communication link to improve the reliability of network data transmission. Two criterions, receiving rate and average delay, can best reflect the quality of links and performance of fault tolerance. The receiving rate of the packet is defined as the ratio of packets received at sink node and packets sent to source nodes. The closer to 1 the packet receiving rate is, the higher qualities of the links are. The average delay of the packet transmission is defined as average delay of all the packets received at sink node from the source nodes.

The fault nodes in network are supposed to be the ones in which the energy consumption reaches the initial threshold value, and the network is based on the model of timing acquisition transmission. CPEQ presented in [15] is the representative of the fault tolerance in multilayer joint optimization and shows the better performance by the comparison with DD (directed diffusion) routing algorithm. Therefore, we will make a comparison of the algorithm presented in this paper with CPEQ in [15] in receiving rate and average packet delay, as shown in Figures 12 and 13.

Figure 12 shows the comparison of the presented algorithm and CPEQ in the packets receiving rate. Fewer fault nodes have arisen before 300 times of the network operation. It cannot show the apparent influence on the performance of the network by them; so we choose the sampling data during the 300–800 times. Along with the increase of operation times, the fault nodes' number also increases. The proposed algorithm has a better performance in packet receiving rate and reflects the good stability in data transmission. Figure 13 shows the comparison of the average packet transmission delay during the operation 300–800 times between the presented algorithm and CPEQ. The newly established transmission route reestablishes the route not from the source node to sink node but from the node ahead of fault node to the sink node by the selection probability. Simulation
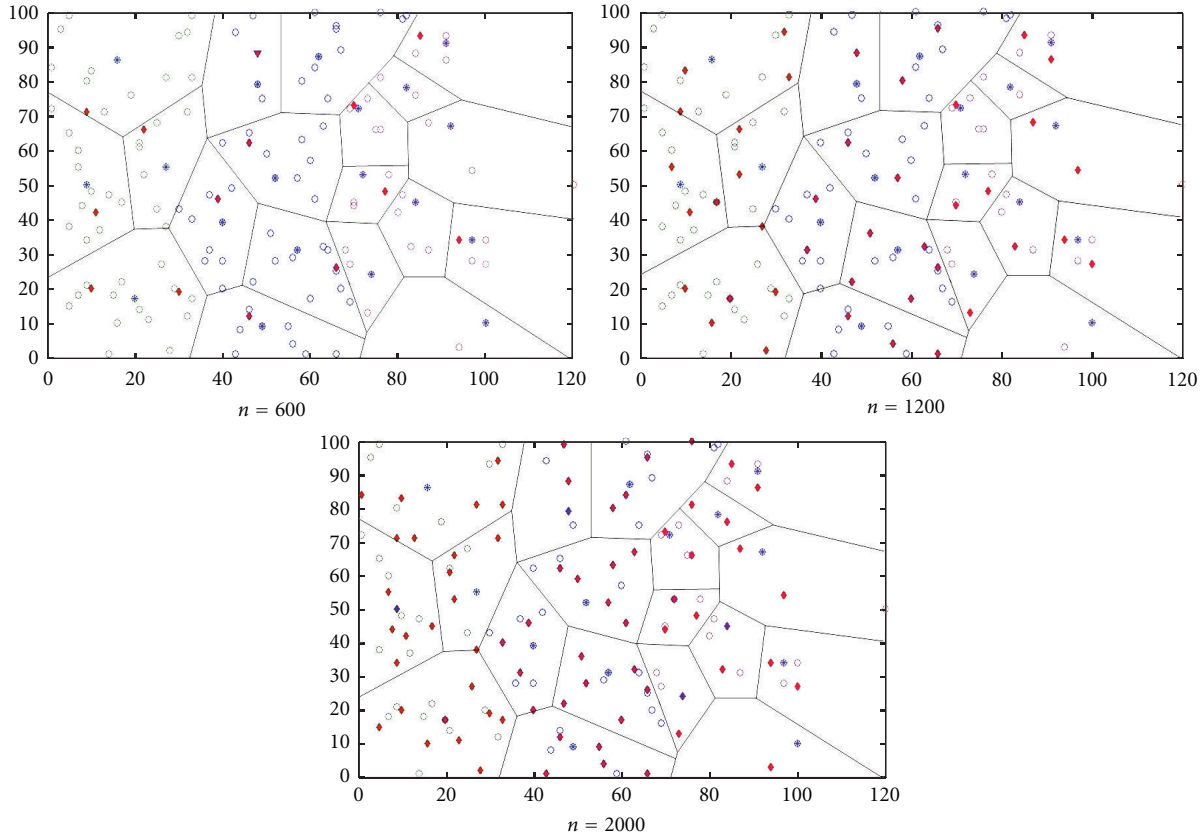
$n = 600$

$n = 1200$

$n = 2000$

FIGURE 15: Energy consumption by nonequal probability and hierarchical clustering.

shows the better performance in average data transmission delay than CPEQ.

4.5. Analysis of Energy Consumption. The routing has been established based on BWAS according to two different clustering models. The first clustering model is equal probability clustering based on IPSO among the nodes with same hierarchy property. The second clustering model is the nonequal probability clustering based on the same BWAS in three hierarchies that different clustering probability is adopted in different hierarchy. Now we do the comparative analysis of energy consumption of the nodes, as shown in Figures 14 and 15.

Figure 14 shows the energy consumption by equal probability and nonhierarchical clustering. Figure 15 shows the energy consumption by nonequal probability and hierarchical clustering. There are total 150 nodes in the network. The red diamond point represents that the sensor node runs out of energy. We analyze the energy consumption at cycle $n = 600$, 1200, and 2000 times. From Figures 14 and 15, the number of dead nodes is, respectively, 21, 44, 96, and 14, 39, 72 when two models run at time $n = 600$, 1200, and 2000. The second model shows the relative smaller number of dead nodes. The dead nodes also represent randomly uniform distribution. It overcomes the "hot" issues in energy consumption caused by equal-probability clustering in WSN.

5. Conclusion and Prospect

In this paper, a fault-tolerant routing algorithm is presented based on the nonuniform hierarchical clustering inspired by the characteristics of vascular network. We build the mathematical model and the topology by marking the nodes with different hierarchies. Nonuniform hierarchical clustering is done based on IPSO with different clustering probabilities in different hierarchical areas. It establishes multiple transmission paths between the neighbor hierarchical nodes by the normalized values of the paths' pheromone generated in BWAS as the path selection probability. It selects the path with maximum probability as the actual data transmitting path to establish the fault-tolerant routing.

Theoretical analysis and simulations show that the topology based on the hierarchical nonuniform clustering can balance the nodes' energy consumption and avoid the hot issue. The routing has higher packets receiving rate and lower average transmission delay. It can avoid the data loss due to the fault of the nodes or links. So it has a good performance in the fault-tolerance and stability of the data transmission.

Our work introduces the characteristics of the vascular network into the fault-tolerant routing for WSN and carries out the studies within the framework of the biological mechanism. As a novel routing algorithm, in-depth study

is needed in the theoretical framework and practical application, especially when it applies to the fault detection and tolerance by the vascular model and the mechanism of the immune system and blood test.

Acknowledgments

References

[1] I. F. Akyildiz, W. Su, Y. Sankarasubramaniam, and E. Cayirci, "Wireless sensor networks: a survey," *Computer Networks*, vol. 38, no. 4, pp. 393–422, 2002.

[2] J. Yick, B. Mukherjee, and D. Ghosal, "Wireless sensor network survey," *Computer Networks*, vol. 52, no. 12, pp. 2292–2330, 2008.

[3] L. Paradis and Q. Han, "A survey of fault management in wireless sensor networks," *Journal of Network and Systems Management*, vol. 15, no. 2, pp. 171–190, 2007.

[4] X. Wang, G. Xing, Y. Zhang, C. Lu, R. Pless, and C. Gill, "Integrated coverage and connectivity configuration in wireless sensor networks," in *Proceedings of the 1st International Conference on Embedded Networked Sensor Systems (SenSys '03)*, pp. 28–39, November 2003.

[5] R. A. F. Mini, A. A. F. Loureiro, and B. Nath, "The distinctive design characteristic of a wireless sensor network: the energy map," *Computer Communications*, vol. 27, no. 10, pp. 935–945, 2004.

[6] R. Badonnel, R. State, and O. Festor, "Management of mobile ad hoc networks: information model and probe-based architecture," *International Journal of Network Management*, vol. 15, no. 5, pp. 335–347, 2005.

[7] H. Alwan and A. Agarwal, "A survey on fault tolerant routing techniques in wireless sensor networks," in *Proceedings of the 3rd International Conference on Sensor Technologies and Applications (SENSORCOMM '09)*, pp. 366–371, June 2009.

[8] P. Djukic and S. Valaee, "Minimum energy fault tolerant sensor networks," in *Proceedings of the IEEE Global Telecommunications Conference Workshops (GLOBECOM '04)*, pp. 22–26, December 2004.

[9] N. M. Hoang and V. N. Son, "Disjoint and braided multipath routing for wireless sensor networks," in *Proceedings of the International symposium on Electrical & Electronics Engineering*, pp. 11–12, 2005.

[10] Y. Challal, A. Ouadjaout, N. Lasla, M. Bagaa, and A. Hadjidj, "Secure and efficient disjoint multipath construction for fault tolerant routing in wireless sensor networks," *Journal of Network and Computer Applications*, vol. 34, no. 4, pp. 1380–1397, 2011.

[11] T. A. Babbitt, C. Morrell, B. K. Szymanski, and J. W. Branch, "Self-selecting reliable paths for wireless sensor network routing," *Computer Communications*, vol. 31, no. 16, pp. 3799–3809, 2008.

[12] R. Luigi, "Effective erasure codes for reliable computer communication protocols," *Computer Communication Review*, vol. 27, no. 2, pp. 24–36, 1997.

[13] P. Djukic and S. Valaee, "Reliable packet transmissions in multipath routed wireless networks," *IEEE Transactions on Mobile Computing*, vol. 5, no. 5, pp. 548–559, 2006.

[14] S. Dulman, S. Nieberg, J. Wu, and P. Havinga, "Trade-off between traffic overhead and reliability in multipath routing for wireless sensor networks," *Wireless Communications and Networking*, no. 3, pp. 1918–1922, 2003.

[15] A. Boukerche, R. Werner Nelem Pazzi, and R. Borges Araujo, "Fault-tolerant wireless sensor network routing protocols for the supervision of context-aware physical environments," *Journal of Parallel and Distributed Computing*, vol. 66, no. 4, pp. 586–599, 2006.

[16] T. Bokareva, N. Bulusu, and S. Jha, "SASHA: toward a self-healing hybrid sensor network architecture," in *Proceedings of the 2nd IEEE Workshop on Embedded Networked Sensors (EmNetS-II '05)*, pp. 71–78, May 2005.

[17] A. Jabbari and W. Lang, "Advanced bio-inspired plausibility checking in a wireless sensor network using Neuro-immune systems: autonomous fault diagnosis in an intelligent transportation system," in *Proceedings of the 4th International Conference on Sensor Technologies and Applications (SENSORCOMM '10)*, pp. 108–114, July 2010.

[18] B. Atakan and O. B. Akan, "Immune system based distributed node and rate selection in wireless sensor networks," in *Proceedings of the 1st Bio-Inspired Models of Network, Information and Computing Systems (BIONETICS '06)*, December 2006.

[19] T. Rui, L. Kenji, and Z. Bing, "Immune system inspired reliable query dissemination in wireless sensor networks," in *Proceedings of the 10th International Conference on Artificial Immune Systems*, pp. 282–293, 2011.

[20] Y. J. Chen, S. F. Yuan, J. Wu, and Y. J. Zhang, "Performance optimization for wireless sensor networks based on immune system," *Systems Engineering and Electronics*, vol. 32, no. 5, pp. 1065–1069, 2010.

[21] Y. Hu, Y. Ding, and K. Hao, "An immune cooperative particle swarm optimization algorithm for fault-tolerant routing optimization in heterogeneous wireless sensor networks," *Mathematical Problems in Engineering*, vol. 2012, Article ID 743728, 19 pages, 2012.

[22] Q. Li, B.-H. Zhang, L.-G. Cui, Z. Fan, and A. V. Vasilakos, "Immunizations on small worlds of tree-based wireless sensor networks," *Chinese Physics B*, vol. 21, no. 5, Article ID 050205, 2012.

[23] H. M. Salmon, C. M. de Farias, P. Loureiro et al., "Intrusion detection system for wireless sensor networks using danger theory immune-inspired techniques," *International Journal of Wireless Information Networks*. In press.

[24] K.-I. Goh, G. Salvi, B. Kahng, and D. Kim, "Skeleton and fractal scaling in complex networks," *Physical Review Letters*, vol. 96, no. 1, 2006.

[25] I. Ahmed, M. Peng, and W. Wang, "Energy efficient cooperative nodes selection in wireless sensor networks," in *Proceedings of the International Conference on Parallel Processing Workshops (ICPPW '07)*, p. 50, September 2007.

[26] I. Ahmed, M. Peng, W. Wang, and S. I. Shah, "Joint rate and cooperative MIMO scheme optimization for uniform energy distribution in Wireless Sensor Networks," *Computer Communications*, vol. 32, no. 6, pp. 1072–1078, 2009.

[27] S. Lindsey, C. Raghavendra, and K. M. Sivalingam, "Data gathering algorithms in sensor networks using energy metrics," *IEEE Transactions on Parallel and Distributed Systems*, vol. 13, no. 9, pp. 924–935, 2002.